Heliyon 11 (2025) e41652

Contents lists available at ScienceDirect

Heliyon

journal homepage: www.cell.com/heliyon

Research article

Encapsulation of bioactive compounds from *Sargassum ilicifolium*: Influence of wall material type and loading content on the physicochemical and structural properties of microparticles

Seyed Saeed Sekhavatizadeh [a], Mohammad Ganje [b,c,*], Seyedeh Sedigheh Hashemi [c], Mohammad Reza Mozafarian [c]

[a] *Department of Food Science and Technology, Fars Agricultural and Natural Resources Research and Education Center, AREEO, Shiraz, Fars, Iran*
[b] *Department of Agriculture, Minab Higher Education Center, University of Hormozgan, Bandar Abbas, Iran*
[c] *Department of Food Science and Technology, Kherad Institute of Higher Education, Bushehr, Iran*

ARTICLE INFO

Keywords:
Chitosan
Encapsulation
Structural properties
WPI
Maltodextrin

ABSTRACT

Sargassum brown seaweed (*Sargassum ilicifolium*) is reported to exhibit several biological activities that promote human health, but it does not have the ability to withstand harsh environmental conditions, such as high temperatures and oxygen exposure. Encapsulation of *Sargassum ilicifolium* extraction through different techniques is known to, optimize physicochemical properties, biological activities, maintain stability, and is an effective way to improve the shelf life of different foods. In the present study, the encapsulation of SIE was carried out by the freeze-drying method using maltodextrin, whey protein isolate (WPI), and chitosan. The bioactive compound of SIE, encapsulation efficiency, and the structural properties of microparticles were analyzed. The evaluations indicated carotenoid (0.77 ± 0.22 mg/g), phenol (0.12 ± 0.02 mg/mL), and flavonoid compounds (4.03 ± 0.28 mg GA/Eg) in the extract, respectively. According to the results, the mixtures of algae extracts prepared with the combination of WPI and MD were more stable and had a lower viscosity than the other treatments. The highest (99.26 %) and lowest (13.41 %) encapsulation efficiencies were obtained for WPI (30 %), MD (70 %), with a 1:12 ratio of SI to wall, and chitosan, with a 1:8 ratio of SI to wall, respectively. X-ray diffraction (XRD), Fourier transform infrared spectroscopy (FTIR), and Scanning electron microscopy (SEM) confirmed the entrapment of the SIE in the beads. Finally, the improved stability and solubility characteristics of the SIE powder, which is based on WPI and maltodextin, indicate its potential for use as a potent functional food additive.

1. Introduction

Macroalgae, commonly known as seaweed, are useful nourishments and restorative herbs in Asian nations [1]. *Sargassum* spp. grow in subtidal and intertidal zones, and their biological flow is affected by water temperature, tidal level, water development, and substrate sorting [2]. *Sargassum ilicifolium* (SI) is found on the Chabahar coast in southeastern Iran and is rich in minerals, fatty acids, vitamins, proteins, and polysaccharides [3]. Various biological functions are associated with seaweeds, including antitumor,

* Corresponding author. Department of Agriculture, Minab Higher Education Center, University of Hormozgan, Bandar Abbas, Iran.
E-mail address: mohammadganje@hormozgan.ac.ir (M. Ganje).

https://doi.org/10.1016/j.heliyon.2025.e41652
Received 8 September 2024; Received in revised form 28 December 2024; Accepted 2 January 2025
Available online 3 January 2025

anti-obesity, antibacterial, antioxidant, anticancer effects; also, delaying Alzheimer's disease, as well as their biological, antimicrobial, anti-inflammatory, and neuroprotective effects [4]. The SI contains a variety of beneficial nutrients, including carbohydrates, essential amino acids, omega-3 and omega-6 fatty acids, antioxidants, beta-carotene, minerals, and vitamins. The concentrations of polysaccharides and essential amino acids within macroalgae vary significantly, with the presence of polysaccharides and phenolic compounds (aromatic compounds) in specific species potentially influencing protein digestibility. Aromatic compounds are secondary metabolite products that are synthesized through the phenylpropanoid and shikimic acid pathways [3]. Phenolic compounds are unstable under harsh conditions and environments. One possible explanation for the significant reduction in aromatic compound stability from the gastric to the intestinal phase could be related to the instability of these compounds, which occurs as a result of the enzymatic hydrolysis of them and the formation of intermediate molecules (quinones or chalcones) that decrease alkaline pH stability [5]. During gastrointestinal digestion, the instability of phenolic extracts has prompted the advancement of technologies aimed at preserving their bioactivity. One such exemplary method is encapsulation [6].

Moreover, the encapsulation technique represents an appropriate choice because it involves gently releasing and exposing bioactive ingredients, inhibiting ion chelation, covering undesirable sensory properties, preventing astringent taste, and protecting phenolic compounds [7].

One of the encapsulation techniques that shows excellent properties in encapsulation is emulsion. Emulsions have a delivery system that involves focused distribution and regulated release of bioactive compounds. The most important factors influencing the release, stability, bioavailability, and absorption of bioactive compounds in various emulsion delivery systems include dispersion conditions, droplet size, oil composition, density, structure of the interface, and the volume fraction [8]. In our previous study, lemongrass extract, black caraway, green coffee, and chavil were microencapsulated via the emulsion technique and then added to kashk, kolompeh, and UF-feta-type cheeses, respectively [9–12].

Generally, polysaccharides and proteins can be used as native carrier agents to integrate core materials. One of the most common encapsulation techniques used for powder production is freeze-drying. Both the drying process and the emulsion substantially influence the core covered with wall materials [13]. Reduced pressure conditions and the long process times are major challenges in the freeze-drying method [14].

Native carrier agents are important in encapsulation. The WPI and casein are the main components of milk protein concentrate (MPC). Caseins are rigid spheres that have a hydrophilic surface and hydrophobic interior, and casein micelles exhibit an open, dynamic structure and a hydrophobic state in milk, allowing the incorporation of whey proteins into micelles [15].

One of the other native carriers characterized as natural biopolymers with excellent biological properties, such as biocompatibility, biodegradability, and hydrophilicity, is chitosan (CS). Because of its natural extracellular matrix, it has been applied in electrospinning encapsulation [8].

MDs are categorized as hydrolyzed starches derived from potatoes, wheat, and corn. Maltodextrins (MDs) are categorized into different groups based on their varying levels of dextrose equivalence. MD with dextrose equivalents ranging from 10 to 20 is widely used because of its easy biodegradability, flavorless formation of encapsulated products, high capacity for low viscosity, ability to absorb water, excellent ability to provide a cost-effective method, and oxidation stability. This technique is subject to certain limitations, the most significant of which include its inadequate emulsifying ability and minimal retention of volatile compounds. Therefore, it is often combined with a variety of other wall materials, such as MPC, to produce stable emulsions [16].

In one study, MD in combination with MPC was used for the encapsulation of *Moringa stenopetala* leaf extract. The efficiency of microencapsulation increased from 83.52 % to 87.93 % for a single encapsulating material and combination, respectively [17].

We hypothesized that SI can be encapsulated with MD in combination with MPC and that CS alone can improve the antioxidant properties of fish oil. To the best of our knowledge, no investigations have been done on the encapsulation of brown algae with the mentioned wall materials. Therefore, the goal of this study was to assess the physicochemical properties of the beads and measure their oxidation parameters.

2. Materials and methods

2.1. Chemicals

Folin–Ciocalteu phenol reagent, amonium thiocyanate, HCl, FeCl3, methanol, Para-ansidin, MD, acetic acid, iso-octane, sodium carbonate, sodium thiosulfate, and chloroform were provided by Merck (Darmstadt, Germany). Tween 80 was purchased from Sigma Aldrich Chemical Co., Gallic acid and standard reagents were obtained from Acros Organics (New Jersey, USA). WPI was supplied by Kalleh Industries, Tehran, Iran.

2.2. Extraction

The *Sargassum ilisifulium* was collected from the coastal area of the Persian Gulf (Hormozgan, Bushehr provinces, Iran). To remove mud and other pollutants, it was washed first with seawater and then fresh water. The sample was kept at 4 °C until it was delivered to the laboratory. For identification of *Sargassum ilisifulium,* the sample was affixed to the herbarium sheet for genus and species identification and deposited in the Algal Herbarium of Agriculture and Natural Resources Studies Center of Hormozgan. The samples were kept in the refrigerator until analysis. Algae was dried on a 6 kg scale in an oven at a temperature of 40 °C overnight. The dried algae samples were powdered in a mill and mixed with 100 % acetone at a ratio of 10 to 1 (w/v) to extract the pigment. The mixture was centrifuged for 10 min at 3000 g to separate the pigment. Then, the extract was passed through a paper filter and concentrated using a

Table 1
Treatments used to formulation of microcapsules.

Treatment code	Maltodexterin (%)	WPI (%)	Chitosan (%)	Wall:SIE ratio
A	50	50	0	4:1
B	50	50	0	8:1
C	50	50	0	12:1
D	30	70	0	4:1
E	30	70	0	8:1
F	30	70	0	12:1
G	70	30	0	4:1
H	70	30	0	8:1
I	70	30	0	12:1
M	0	0	10	4:1
N	0	0	20	8:1
O	0	0	30	12:1

rotary evaporator at a temperature of 30 °C. In the next step, 2 g of anhydrous sodium sulfate was used to remove excess water. Finally, the pigments were stored in a glass container filled with inert nitrogen (−20 °C) in a dark place until use [18]. All the equipment and utensils required were autoclaved and placed in 1 % hydrochloric acid for 24 h, and then washed twice with sterile distilled water.

2.3. Chlorophyll pigments, carotenoid, and total flavonoid content

To measure chlorophyll, Mohammadi Kabari's (2024) method was used. First, 3 g of SI was added to 12 mL of acetone 80 % in a low-light environment and cool place. The extracted solution was filtrated through a Whatman's paper No. 42 and acetone 80 % was used for 50 mL adjustment. The absorbance of the extract was then read at 663 and 645 nm for chlorophyll (a, b), and at 480 and 663 for carotenoids, with a Shimadzu UV-120-02 spectrophotometer (Japan). The following equations were used to calculate chlorophyll *a* (Eq. (1)), chlorophyll *b* (Eq. (2)), total chlorophyll (Eq. (3)) and carotenoid (Eq. (4)) [19].

$$\boldsymbol{Chl_{(a)} = 0 \cdot 0127 A_{663} - 0 \cdot 00269 A_{645}} \quad \text{Eq. 1}$$

$$\boldsymbol{Chl_{(b)} = 0 \cdot 0229 A_{645} - 0 \cdot 00468 A_{663}} \quad \text{Eq. 2}$$

$$\boldsymbol{Chl_{(a+b)} = 0 \cdot 0202 A_{645} + 0 \cdot 00802 A_{663}} \quad \text{Eq. 3}$$

$$\boldsymbol{Cartenoid(mg / g\ SI) = \frac{7 \cdot 6 A_{480} - 1 \cdot 49 A_{510}}{v \times 1000}} \quad \text{Eq. 4}$$

When: A is adsorption, V is sample volume.

The total flavonoid content was evaluated following the methodology established by Ghanbarzadeh et al. (2009), which involved the formation of a flavonoid-aluminum complex.

One mL of methanolic extract or standard flavonoid compound (Quercetin) was combined with 4.0 mL distilled water and 0.3 mL $NaNO_2$ and left in the dark for 6 min.

Following the initial mixture preparation, 1.0 mL 10 % $AlCl_3.6H_2O$ was incorporated and the solution was incubated under dark conditions for 5 min to ensure the completion of the reaction. After this period, 2 mL of 1.0 M NaOH and distilled water were introduced to achieve a final volume of 10 mL. The absorbance of the resulting solution was measured at 510 nm using a spectrophotometer. The flavonoid content was expressed as mg quercetin equivalent (QE) per gram of sample net weight [20].

2.4. Evaluation of antioxidant properties

To evaluate the antioxidant activity of the *sargassum* acetone extract, 2 mL of DPPH (100 μM) dissolved in methanol was mixed with 2 mL of different concentrations of algae extract; the mixture was placed in a dark place for 30 min. The absorbance of the sample was immediately measured at a wavelength of 520 nm with a spectrophotometer and the antioxidant activity was calculated using Eq. (5) (Sun et al., 2007).

$$\%\ \text{Radical scavenging} = \left(1 - \frac{\text{Abs} \cdot \text{sample}}{\text{Abs} \cdot \text{control}}\right) \times 100 \quad \text{Eq. 5}$$

Abs. control is the absorbance of the DPPH solution without sample and Abs sample is the absorbance of the control samples.

2.5. Preparation of beads

The MD, WPI, and CS wall material solutions were prepared by their different concentrations in distilled water (Table 1). The polymer molecules were fully hydrated by leaving the solutions at room temperature overnight. As a carrier oil, canola oil was mixed

with SIE (Carrier oil: SIE ratios were 1:1) and then 1 g emulsifier (Tween 80) was added to the solution. The SIE was added in three different cores coating ratios: (1:4), (1:8), and (1:12). Then, the mixtures were homogenized (pre-homogenized) in Ultra-Turrax homogenizer at 12000 rpm for 10 min. Samples were treated with an ultrasonic homogenizer (Eurosonic 4D, Italy) at 300 W power, 50 kHz frequency, for 1 min after the high-speed homogenization process. During the ultrasound, samples were kept in an ice bath for protection. To desiccate beads a freeze dryer (Freeze-dryer FD-5003-BT, Dena Vacuum, Iran) was used for 12 h.

2.6. Creaming index (CI) measurement

Ten mL of sample was added to a 250 mL Lab Glass Cylinder. The opaque cream and serum layer were measured after leaving the sample undisturbed for 24 h. Finally, the CI index was calculated according to Eq. (6) [21]:

$$CI(\%) = \left(\frac{H_{sample}}{H_{total}}\right) \times 100 \quad \text{Eq. 6}$$

2.7. Viscosity

To measure viscosity, a rheometer (MCR 302, Anton Paar, Austria) was used. The samples (10 %, w/v_{DW}) were were left untouched for 12 h before viscosity measurement. The sample (5 mL) was placed in a concentric cylinder geometry at 23 °C and exposed to a shear rate ranging from 10 to 100/s.

2.8. Bulk density (BD) and total phenol

To determine BD, 2 g of bead powder was added to a 50 mL graduated cylinder. The bulk density was determined by taking the ratio of the powder mass to the volume it occupied within the cylinder [22].

The phenolic compounds (TPC) of the samples were quantified following the Folin–Ciocalteu method outlined by McDonald et al. (2001), and reported as gallic acid equivalents (GAE) in milliequivalents per gram dry material. This led to the formation of a blue complex that exhibits peak absorption at 760 nm.

2.9. Solubility

For solubility assessment, 2 g of sample was added to 30 mL of distilled water with continuous stirring for 30 min at 700 rpm on a magnetic stirrer. It was then centrifuged at 6000 rpm for 30 min. The collected supernatant was dried in an oven at 105 °C for 5 h. The weight of the sediment in the tube after centrifugation was also measured [23]. Water solubility was then determined using Eq. (7):

$$water\ solubility = \frac{Dried\ supernatant\ weight}{sample\ weight} \times 100 \quad \text{Eq. 7}$$

2.10. Encapsulation efficiency

Encapsulation efficiency is determined by measuring phenolic compounds. The microencapsulated powder (800 mg) was accurately weighed, added to 4 mL of methanol (as solvent), and gently vortexed for 2 min at room temperature. The tubes were then placed in a centrifuge (IEC Centra-3 M Centrifuge, UK) for 5 min at 3000 rpm. The Folin-Ciocalteu colorimetric method was used for measuring phenolic compounds in the beads, and finally called microencapsulated polyphenols (mgGA/g beads). For dried SIE polyphenol content in each formulation, the Folin-Ciocalteu colorimetric method was used, and the result was recorded based on the (mg GA/g $_{SIE}$ used in the formulation). Therefore, the EE% was calculated using Eq. (8) [24].

$$EE\ (\%) = \frac{Microcapsulated\ Total\ phenol}{Extracted\ Total\ phenol\ that\ used\ in\ formulation} \times 100 \quad \text{Eq. 8}$$

2.11. Particle size distribution and zeta potential

A dynamic light scattering (DLS) instrument (SZ-100, Horiba Ltd., Kyoto, Japan) was used to determine the intensity-weighted average droplet size at the target temperature of 25 °C and scattering angle of 90°. One gram of beads was suspended in 100 mL of deionized water. Then, 1 mL of the suspension was placed in a polycarbonate cuvette (Quartz glass cuvette 2 opening). After bead dispersion, the refractive index 1.3326, as the standard material polystyrene latex, was chosen. The SZ-100 software for Windows was applied for Data analysis. For calculation, the standard mode was chosen. ND filter was adjusted in automatic mode. The focus position in the center and the detector position at 173° angle were adjusted.

2.12. Scanning electron microscopy (SEM)

Freeze-dried samples were fixed in an aluminum holder and covered with gold using a spray coater (Desk Sputter CoaterDSR1, Nano Structural Coating Co., Iran). They were used for the preparation of the SEM sample. Scanning electron microscope (SEM,

Table 2
Chemical composition values of sargassum algae (*Sargassum ilisifolium*).

Compounds	Concentration
Chlorophyll *a*	1.90 ± 0.62 mg/g
Chlorophyll *b*	2.83 ± 0.17 mg/g
Chlorophyll *b*+a	4.73 ± 0.28 mg/g
Carotenoid	0.77 ± 0.22 mg/g
Total phenol	0.12 ± 0.02 mg/ml
Total flavonoid	4.03 ± 0.28 mgGA/Eg
DPPH	9.63 ± 0.45 mgGA/Eg

Table 3
Creaming index and viscosity for microencapsulated emulsions of *Sargassum ilisifolium*.

Treatment code	Creaming Index	Viscosity
M	10 ± 0.50^{c}	70.53 ± 1.40^{b}
N	10 ± 0.60^{c}	106.5 ± 1.66^{a}
O	10 ± 0.20^{c}	68.88 ± 1.05^{c}
D	20 ± 0.30^{b}	12.28 ± 0.13^{f}
E	5 ± 0.20^{e}	4.25 ± 0.12^{i}
F	25 ± 1.0^{a}	4.79 ± 0.12^{hi}
G	10 ± 0.80^{c}	4.94 ± 0.13^{hi}
H	5 ± 0.70^{e}	6.50 ± 1.26^{d}
I	21 ± 1.00^{b}	6.44 ± 0.19^{g}
A	10 ± 0.50^{c}	14.45 ± 0.16^{e}
B	10 ± 0.20^{c}	11.39 ± 0.12^{f}
C	8 ± 0.50^{d}	6.17 ± 0.12^{gh}

* Data are reported as (mean ± standard deviation) in three replicates.
**The same lowercase letters in each column row indicate no significant difference ($P > 0.05$) between the data based on Duncan's test.
***(A): Maltodexterin (50 %) + WPI (50 %) - 4:1; (B): Maltodexterin (50 %) + WPI (50 %) - 8:1; (C): Maltodexterin (50 %) + WPI (50 %) - 12:1; (D): Maltodexterin (30 %) + WPI (70 %) - 4:1; (E): Maltodexterin (30 %) + WPI (70 %) - 8:1; (F): Maltodexterin (30 %) + WPI (70 %) - 12:1; (G): Maltodexterin (70 %) + WPI (30 %) - 4:1; (H): Maltodexterin (70 %) + WPI (30 %) - 8:1; (I): Maltodexterin (70 %) + WPI (30 %) - 12:1; (M): Chitosan (10 %) - 4:1; (N): Chitosan (10 %) - 8:1; (O): Chitosan (10 %) - 12:1.

VEGA3, TESCAN, Czech Republic) is used for observation of sample pictures. The accelerating voltage was 10.0 kV. The working distance between the sample surface and the microscope objective was 7.03–8.91 mm.

2.13. Fourier transform infrared spectroscopy (FTIR)

FTIR analysis was performed using FT/IR-4100 equipment (Rayleigh, WQF-510A, China), equipped with a diamond single reflection attenuated total reflectance (ATR) module. Samples were scanned with a spectral resolution of 4 cm^{-1} in the spectral interval 450–4000 cm^{-1}.

2.14. X-ray diffraction (XRD)

Crystal structure analysis was done by X-ray diffractometer (XRD) analysis. The conditions for conducting this test were a voltage of 40 kV and a current of 30 mA. Bead powder samples were loaded on an aluminum plate and X-ray diffraction profiles. The range of diffraction angles (2θ) was 10–80 with a scanning speed of 0.02 per min.

2.15. Statistical analysis

SPSS (ver. 21) was applied for data analysis. One-way analysis of variance was used for statistical data analysis. To find the significant ($p \leq 0.05$) difference between the means values, Duncan post-hoc test was used.

3. Results and discussions

3.1. Chemical compounds and antioxidant properties of sargassum

According to scientific and laboratory studies, brown seaweeds, such as *Sargassum*, have significant phenolic contents, and

consequently, strong antioxidant properties. This is due to their tidal nature and exposure to sunlight, particularly UV-B (280–320 nm) and UV-A (320–400 nm) radiation [25]. The findings from this study indicate that SIE is a suitable source of natural antioxidants, such as carotenoids, phenols, and flavonoids, and demonstrates appropriate antioxidant activity (based on the TBHQ value). The total phenol and flavonoid contents in this study were estimated to be approximately 0.1199 ± 0.02 mg/mL and 4.03 ± 0.28 mg GA/E, respectively. The values of other chemical compounds and pigments in the acetone extract of Sargassum, as well as the free radical scavenging capacity in terms of DPPH, are presented in Table 2, which highlights the antioxidant benefits of this algal species.

3.2. Creaming index (CI)

In the present study, the range of the creaming index in most treatments was between 5 % and 10 %, indicating relatively high stability in most of the prepared treatments. Among these, the highest instability was seen in treatments F and I with approximately 25 % and 21 % separation respectively, had the lowest instability (Table 3). In treatments F and I, the main characteristic was the high ratio of algae to wall materials (12:1), which seemed to affect the emulsifying properties of these compounds at a 70:30 ratio of MD to WPI. According to some studies, the emulsifying capacity of MD is low at high core-to-wall material ratios as a coating [26]. Moreover, alginate exists as a structural component of the cell wall of marine brown algae. It is a linear 1,4- linked copolymer of β-D- mannuronic acid and α-L- guluronic acid. Alginates are essential compounds as thickening, gelling, or stabilizing agents. Consequently, they may affect the emulsifying properties [27].

Typically, the emulsifying property of WPI and MD mixtures is less than that of CS. It has been reported that the droplet size of emulsions resulting from WPC and MD mixtures at a 70:30 ratio is larger than that resulting from treatments prepared with a CS wall [28,29]. In this case, a significant amount of unabsorbed polysaccharide remains in the aqueous phase of the emulsion [29]. The researchers proposed that differences in emulsifying properties may be influencing factors in this process. These properties include the rate of surface adsorption at the droplet interface, surface activity, shape-forming characteristics, and intermolecular interactions at the oil-water interface [12]. Accordingly, the lack of a significant difference in the separation index or stability of emulsions in most treatments can be attributed to the presence of MD in three-quarters of the corresponding emulsifying treatments. Additionally, a study of treatments prepared with a CS wall combination revealed that this wall composition effectively increased the stability of the capsules. Notably, protein particles play an important role in improving and enhancing the properties of emulsions used in the microencapsulation of oils and fats [30]; however, studies on this characteristic concerning algal carotenoids are limited. In a research, inulin-type dietary fibers as emulsion-filled gel were added to clove bud oil rich in eugenol and encapsulated by freeze-drying. Inulin did not enhance creaming stability; rather, it acted as a physical barrier, improving the encapsulation efficiency of eugenol to nearly 100 % [31].

3.3. Viscosity

The results of the viscosity test indicated a significant effect ($p < 0.05$) of different wall materials in most of the treatments studied (Table 3). The highest viscosity index was measured for the CS treatments, especially the N treatment with a ratio of 8:1, and a value of 106.5 ± 1.66 mPa s, which was significantly different from that of the other treatments prepared with the MD and WPI wall combination ($p < 0.01$). The lowest viscosity was observed in treatments E, F, and G, with an approximate value of 4 mPa s.

MD is known as a wall material with low viscosity [32]. Considering its presence in the three treatment combinations at concentrations of 30 %, 50 %, and 70 %, no noticeable change in the viscosity resulting from the combination of MD and WPI at different wall and extract ratios was observed. The lowest viscosity, approximately 4 mPa s, was related to treatments F, I, and E, which were prepared from the aforementioned wall materials at ratios of 70:30, 30:70, and 50:50, respectively.

According to the results presented in Table 3, the effect of CS on viscosity showed a sharp jump compared with other treatments. It has been reported that CS increases the viscosity of food emulsions. Carneiro et al. (2013), in their study on flaxseed oil, reported that the presence of CS resulted in the highest viscosity in the flaxseed oil emulsion. CS is a high-viscosity material with a high absorption capacity. It is generally used as a thickening agent in food products and owing to its active hydroxyl and amino groups, has a strong ability to undergo chemical reactions. These reactions alter its crystalline structure, ultimately increasing its water solubility (Carneiro et al., 2013).

Other studies have also indicated that the use of CS as a wall coating results in the highest viscosity compared with the WPI and MD combination, which aligns with the present research [26,33,34].

Moreover, *Teucrium polium* L. extract was nanoencapsulated with maltodextrin/Persian gum using freeze-drying. The results showed increasing the maltodextrin concentration reduced the viscosity [34]. The findings of this study corroborate the results of our research [35].

3.4. Total phenol content and density

The highest total phenol content was found in treatment I (0.11 ± 0.05 %), which used a wall combination of WPI (30 %) and MD (70 %) at a 12:1 ratio. This was followed by treatment M from the CS wall combination group at a 4:1 ratio, with a value of 0.04 ± 0.01 %; and treatment with C using a combination of WPI (50 %) and MD (50 %) at a 12:1 ratio, and a value of 0.11 ± 0.05 %. Finally, treatment F, with a wall combination of WPI (70 %) and MD (30 %) at a 12:1 ratio, had a value of 0.09 ± 0.02 % (Table 4). In most of the treatments, increasing the extract-to-wall ratio resulted in a higher phenol content in the capsules.

The density varied from 0.02 to 0.44 depending on the type of wall material used, leading to significant differences between the

Table 4
Solubility, total phenol, density and encapsulation efficiency for microencapsulated *Sargassum ilisifolium*.

Treatment Code	Solubility (%)	Total Phenol (mg/ml)	Density (g/ml)	Encapsulation Efficiency (%)
M	84.0 ± 2.90^{c}	0.04 ± 0.01^{c}	0.03 ± 0.01^{f}	39.76 ± 0.64^{g}
N	30.0 ± 2.13^{f}	0.01 ± 0.01^{g}	0.02 ± 0.04^{f}	13.41 ± 1.09^{i}
O	93.33 ± 2.75^{b}	0.03 ± 0.02^{g}	0.05 ± 0.05^{f}	29.42 ± 0.95^{h}
D	93.0 ± 2.15^{b}	0.07 ± 0.03^{ef}	0.20 ± 0.04^{cd}	67.81 ± 0.79^{f}
E	67.5 ± 1.50^{de}	0.08 ± 0.01^{g}	0.20 ± 0.02^{cd}	72.72 ± 1.24^{e}
F	10.2 ± 2.73^{h}	$0.09 \pm 0.02d^{e}$	0.14 ± 0.01^{e}	78.50 ± 0.80^{d}
G	98.0 ± 2.80^{a}	0.11 ± 0.01^{f}	0.20 ± 0.03^{cd}	98.66 ± 0.54^{a}
H	66.6 ± 1.80^{e}	0.10 ± 0.02^{f}	0.44 ± 0.03^{a}	87.99 ± 0.66^{b}
I	65.0 ± 2.50^{e}	0.11 ± 0.05^{b}	0.16 ± 0.02^{de}	99.26 ± 1.40^{a}
A	20.0 ± 2.88^{g}	0.01 ± 0.02^{a}	0.24 ± 0.01^{bc}	83.77 ± 0.73^{c}
B	71.42 ± 2.08^{d}	0.09 ± 0.02^{g}	0.19 ± 0.03^{cde}	79.67 ± 1.03^{d}
C	80.0 ± 2.37^{c}	0.11 ± 0.05^{d}	0.28 ± 0.02^{b}	95.27 ± 1.49^{b}

* Data are reported as (mean ± standard deviation) in three replicates.
**The same lowercase letters in each column row indicate no significant difference ($P > 0.05$) between the data based on Duncan's test.
***(A): Maltodexterin (50 %) + WPI (50 %) - 4:1; (B): Maltodexterin (50 %) + WPI (50 %) - 8:1; (C): Maltodexterin (50 %) + WPI (50 %) - 12:1; (D): Maltodexterin (30 %) + WPI (70 %) - 4:1; (E): Maltodexterin (30 %) + WPI (70 %) - 8:1; (F): Maltodexterin (30 %) + WPI (70 %) - 12:1; (G): Maltodexterin (70 %) + WPI (30 %) - 4:1; (H): Maltodexterin (70 %) + WPI (30 %) - 8:1; (I): Maltodexterin (70 %) + WPI (30 %) - 12:1; (M): Chitosan (10 %) - 4:1; (N): Chitosan (10 %) - 8:1; (O): Chitosan (10 %) - 12:1.

various wall materials. The highest density was observed for microcapsules H and A, with values of 0.44 ± 0.03 and 0.24 ± 0.01 g/mL, respectively. The lowest density was found in the group of microcapsules prepared with a CS wall (Table 4). A higher density can indicate a lower amount of trapped air among the particles, which in turn contributes to greater oxidative stability [36–38].

3.5. Solubility

The solubility of food powders is a critical functional property with significant economic and market appeal. Solubility depends on the particle size and shape, type and concentration of carriers, and drying conditions [39]. The number of water-binding groups in the molecules of each substance determines the solubility of the microencapsulated compounds [40]. In a study by Zhao et al. (2022) on the solubility of microcapsules, the results indicated a significant effect of wall composition changes on the final microcapsule solubility ($P < 0.05$) [41]. In the present study, MD was used as the base compound in three-quarters of the wall material compositions. The results revealed that the highest solubility index, averaging 76 %, was observed in the treatments with 30 % WPI and 70 % MD ratio. In a study by Kaveh et al. (2018) on the physicochemical properties of stevia microcapsules made with MD and WPI as wall materials, the average solubility of the stevia powders was 83.74 % [42]. Increasing the WPI concentration significantly reduced powder solubility. For powders containing MD, increasing the concentration from 10 % to 20 % led to a significant decrease in solubility, but further increases in carrier concentration did not result in significant changes, which aligns with the results of the present study. The results revealed no significant differences in solubility between powders from microencapsulation with various wall materials. In all the treatments with CS walls, the solubility index was closer to the highest average value, similar to the findings of Macías-Cortés et al. (2020) The reduced solubility of some treatments with increasing wall-to-extract ratios of 8:1 and 12:1 can be attributed to the presence of larger particles, resulting in higher adhesion and surface tension [40]. In a study on dried soy milk powder, Syll et al. (2013) reported that particle size and density significantly impact dispensability, with particles ranging from 15 to 24 μm exhibiting the highest solubility and disperse ability. Additionally, the formation of insoluble materials during the drying process and powder adhesion to drying chamber walls can reduce powder solubility [43,44]. The solubility index is a crucial factor in the stability of microencapsulated powders because low solubility can increase particle adhesion, accelerate microbial growth, and expedite oxidation [45]. In similar research, *Capparis spinosa* fruit extract was nanoencapsulated with lecithin and cholesterol. The water solubility of spray-dried beads ranged from 39.5 to 43.7 %. It seemed that decreasing the carbohydrate content and incorporating extract, especially in the form of a nanocapsule, would have a negative effect on the WSI. The findings of the current investigation are consistent with our results [46].

3.6. Encapsulation efficiency

One of the most important criteria for evaluating and confirming the success of encapsulation processes is the use of a microencapsulation efficiency index. The microencapsulation efficiency refers to the amount of core material (with a focus on the total phenol content) encapsulated within the wall [47]. Notably, the microencapsulation efficiency associated with formulations prepared with a combination of WPI and MD was higher than that of CS. This increase can be attributed to the emulsifying property of the WPI and MD combination. It has been reported that the combination of wall materials, especially the combination of proteins and polysaccharides relative to single polymers, provides better emulsifying properties and coverage [48,49].

With an increase in the ratio of WPI to MD in the wall material, the microencapsulation efficiency gradually decreased for all core: wall ratios (Table 4). MD lacks surface-active properties, which can lead to weak wall materials when used alone in encapsulation processes; however, in combination with WPI, which has good emulsifying properties, they form an acceptable wall material

Table 5
Size and zeta potential of microcapsules containing algae extract.

Treatment Code	Particle Size (nm)	Zeta Potential
C	148.7 ± 41.37[b]	−30.4 ± 1.37[c]
F	114 ± 8.45 [b]	−27.7 ± 0.85[b]
I	214.7 ± 13.67[a]	−31.7 ± 0.95[c]
M	37.6 ± 8.13[c]	−57.1 ± 0.20[a]

* Data are reported as (mean ± standard deviation) in three replicates.
**The same lowercase letters in each column row indicate no significant difference (P> 0.05) between the data based on Duncan's test.
*** (C): Maltodexterin (50 %) + WPI (50 %) - 12:1; (F): Maltodexterin (30 %) + WPI (70 %) - 12:1; (I): Maltodexterin (70 %) + WPI (30 %) - 12:1; (M): Chitosan (10 %) - 4:1.

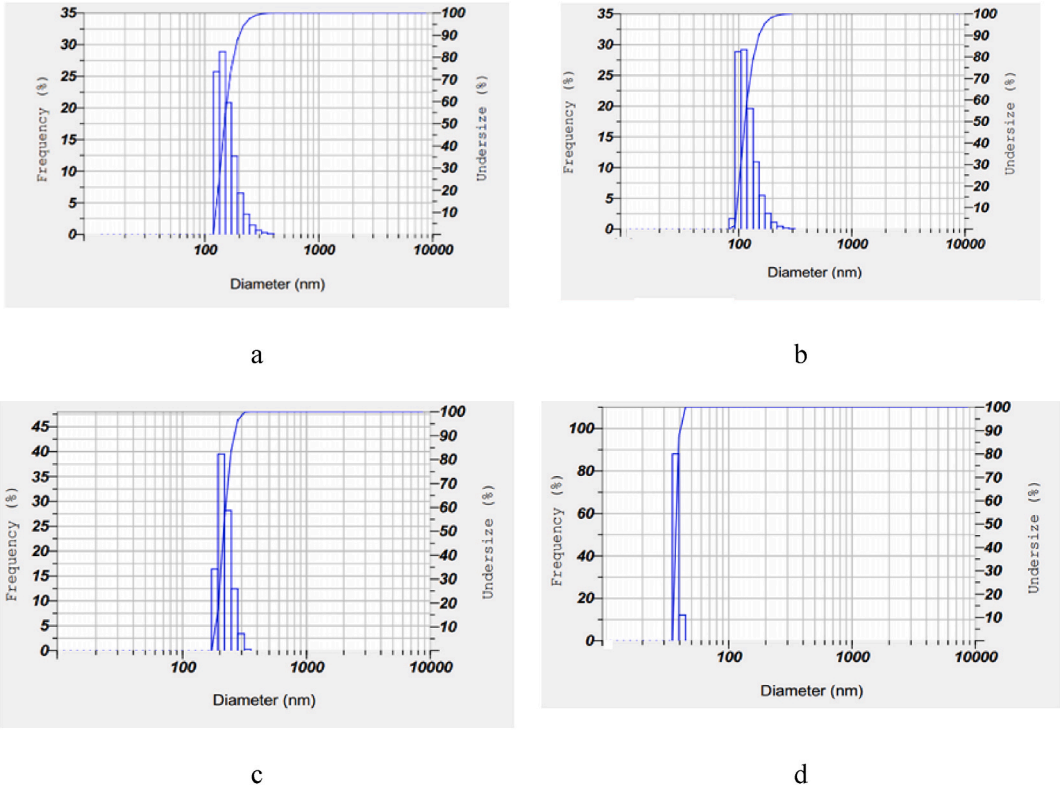

Fig. 1. Droplets size distribution of (a) (C): Maltodexterin (50 %) + WPI (50 %) - 12:1; (b) (F): Maltodexterin (30 %) + WPI (70 %) - 12:1; (c) (I): Maltodexterin (70 %) + WPI (30 %) - 12:1 and (d) (M): Chitosan (10 %) - 4:1.

combination [50,51].

Another reason for the effectiveness of WPI in terms of encapsulation efficiency is that their interaction and absorption at the oil-water interface can alter the protein structure, which can play a significant role in forming a resistant and stable layer around oil droplets [52,53]. This is important because a decrease in microencapsulation efficiency can result from insufficient wall materials for producing a strong matrix, leading to thinner layers of wall materials between emulsion droplets or the instability of these droplets during drying processes [54]. Conversely, improving the microencapsulation efficiency may be due to the rapid formation of a shell on the surface of the particles. Further complementary tests were conducted on the four treatments with the highest encapsulation efficiency: treatment I with a combination of WPI (30 %) and MD (70 %) at a ratio of 12:1; treatment C with a combination of WPI (50 %) and MD (50 %) at a ratio of 12:1; treatment F with a combination of WPI (70 %) and MD (30 %) at a ratio of 12:1; and treatment M from the CS group at a ratio of 4:1. These treatments were selected based on their demonstrated high encapsulation efficiency and the potential benefits of the WPI and MD combination in enhancing microencapsulation effectiveness. In a similar investigation, propolis extract was encapsulated in ovalbumin protein by spray drying. The encapsulation efficiency was 88.20 % [55].

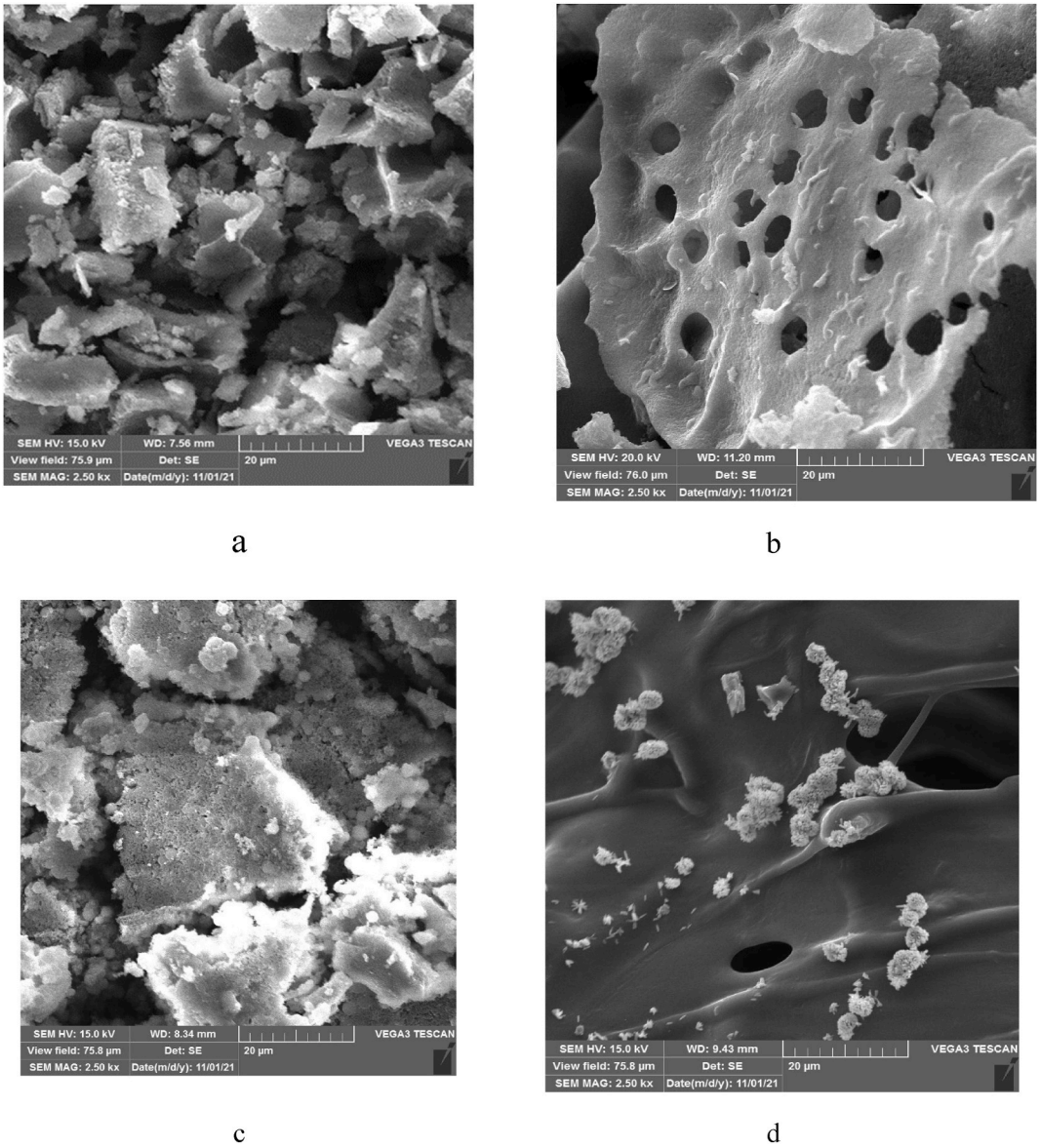

Fig. 2. SEM image of(a) (C): Maltodexterin (50 %) + WPI (50 %) - 12:1; (b) (F): Maltodexterin (30 %) + WPI (70 %) - 12:1; (c) (I): Maltodexterin (70 %) + WPI (30 %) - 12:1 and (d) (M): Chitosan (10 %) - 4:1.

3.7. Particle size and zeta potential

To analyze the particle size and zeta potential of the samples, the four microcapsules with the highest encapsulation efficiency from freeze-drying were examined. The smallest particle sizes were found in treatment M (CS wall material with a ratio of 4:1), treatment F (WPI 30 %) and MD (70 % wall material with a ratio of 12:1). Additionally, the lowest zeta potential was observed in treatment I (WPI (70 %) and MD (30 %) wall materials with a ratio of 12:1) (Table 5).

A review of the results from dynamic light scattering (DLS) and the particle size index revealed that microcapsules produced with WPI and MD as wall materials tended to have larger particle sizes than those produced with CS as the wall material. Furthermore, it was evident that the ratio of WPI to MD in the wall material had a significant relationship with the particle size obtained, such that increasing the ratio of WPI from 30 % to 70 % resulted in a larger particle size.

Fig. 1 shows the particle size distribution curves of the different treatments. Increasing the proportion of WPI to MD in the wall material reduced the breadth of the size distribution curves. This reduction in heterogeneity can be explained by the high emulsifying power of WPI, which leads to more uniform and homogeneous emulsions than MD, known for its weaker emulsifying properties.

Another phenomenon noted in various sources is that increasing the oil concentration in emulsions typically leads to larger particle sizes [56,57]. This is attributed to insufficient protein available for adsorption at the oil-water interface with higher oil concentrations,

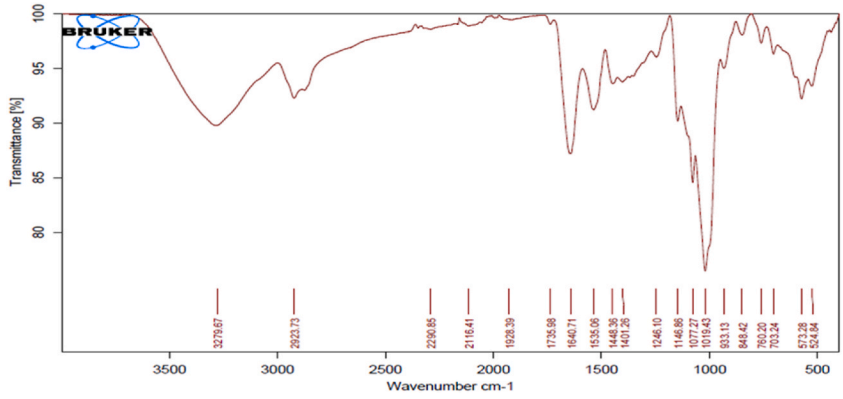

a

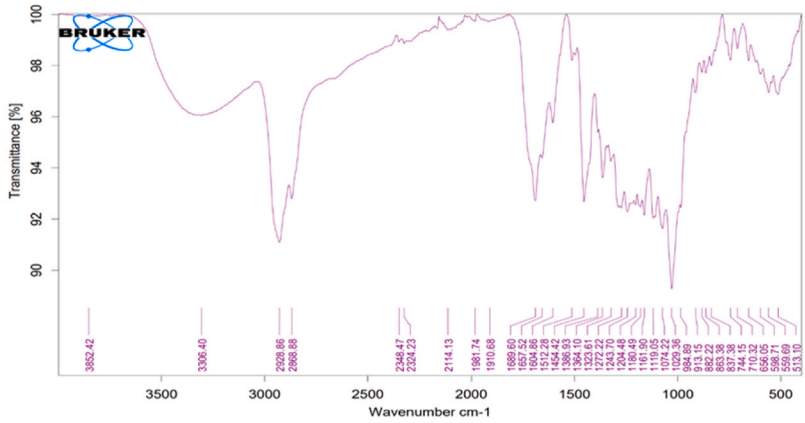

b

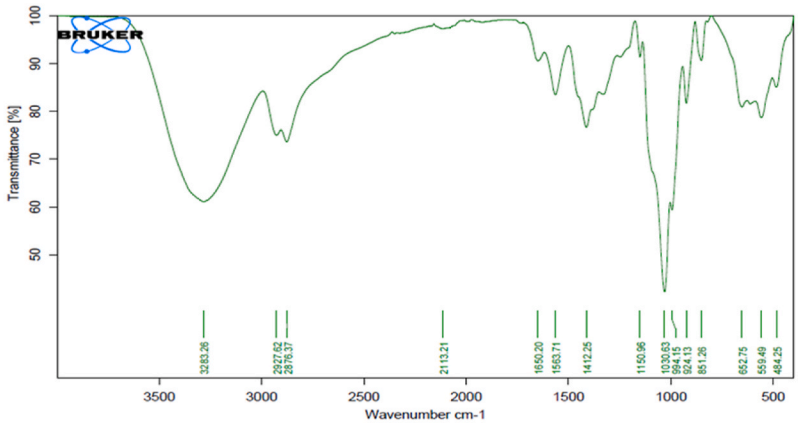

c

Fig. 3. FTIR spectra of (a) Pure extract of Sargassum, (b) (M): Chitosan (10 %) - 4:1) and (c) (C): Maltodexterin (50 %) + WPI (50 %) - 12:1.

resulting in coalescence and larger droplet sizes in the emulsion [58].

The findings of Jafari et al. (2008) indicate a relationship between particle size and encapsulation efficiency, which aligns with the results reported in this study [59]. Specifically, treatment I, prepared with WPI (70 %) and MD (30 %) at a ratio of 12:1, exhibited the highest encapsulation efficiency and total phenol content, despite having the largest particle size according to Tables 4 and 5 Tao et al.

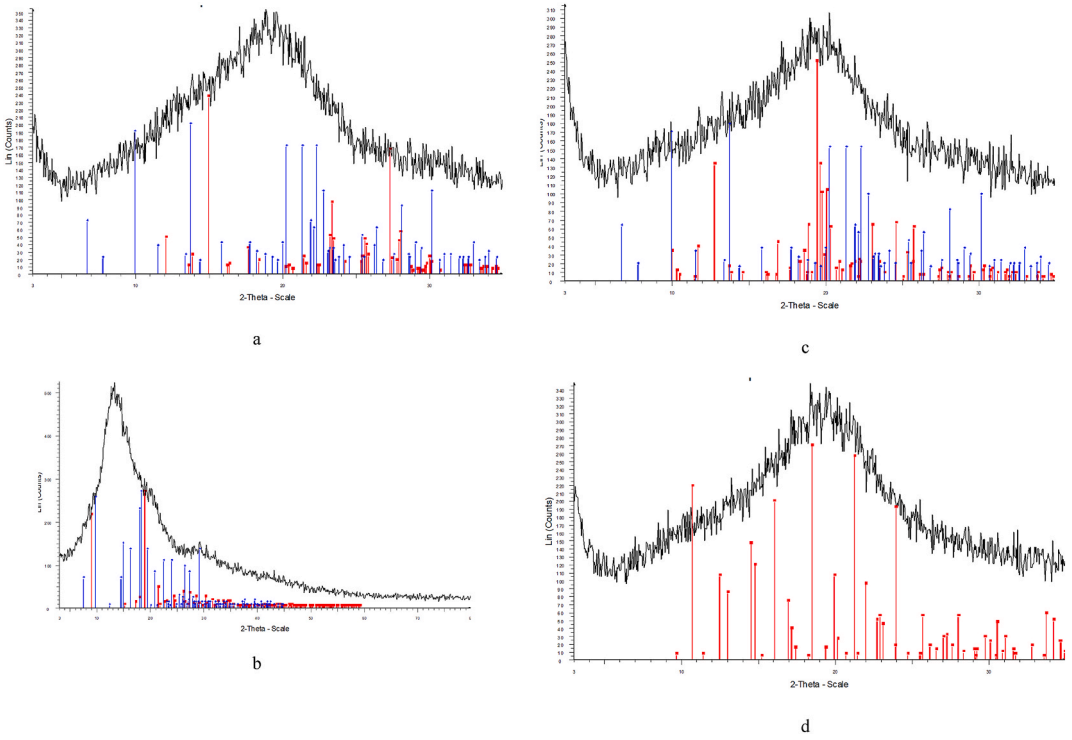

Fig. 4. X-Ray diffraction scans of (a) (C): Maltodexterin (50 %) + WPI (50 %) - 12:1; (b) (F): Maltodexterin (30 %) + WPI (70 %) - 12:1 (c) (I): Maltodexterin (70 %) + WPI (30 %) - 12:1 and (d) (M): Chitosan (10 %) - 4:1).

(2024) encapsulated *Pterostilbene* grapeseed oil emulsion by spray drying. The particle size was 8–19 μm. It was similar to our results [60].

Zeta potential in emulsions serves as a method to determine the amount of electric charge on particles, with highly positive or negative values indicating stability and preventing phase separation in the emulsion. As presented in Table 5, the negative values for the WPI and MD combinations, as well as the significantly positive value for the CS-based capsules, indicate the appropriate stability of the formed emulsions.

3.8. Investigation of the morphological characteristics of the microcapsule particles

To investigate the surface morphology of the microcapsules, scanning electron microscopy (SEM) was used. Among the various treatments with the highest encapsulation efficiency, samples M, I, C, and F were examined under the same magnification. Microcapsules obtained from freeze-drying generally exhibit a layered state, as illustrated in Fig. 2, with an irregular glassy shape. The SEM images revealed the pseudo-sheet-like and glassy microstructure of the powders obtained from microencapsulation as the predominant feature across all optimized treatments. According to the SEM images, the visual structures of the powders obtained from freeze-drying are very similar [61]. In all powder microstructures, significant defects and voids were observed, which was attributed to the formation of small ice crystals during freezing as the primary cause of this phenomenon [62]. Additionally, Ratti (2024) and Laureanti et al. (2023) examined the dried structure of samples and other common drying methods and reported that ice crystals suddenly sublimate after formation during freeze-drying, resulting in irregularities and porous structures on the microcapsules, which is consistent with the findings of the present study. The SEM images clearly show that simultaneously increasing the ratio of WPI to MD significantly reduces the number of surface pores and fractures, resulting in more cohesive and flatter microcapsules. These findings align with the results of a study conducted by Chranioti et al. (2015). This difference can be explained by the high protein concentration in the matrix walls of treatments C (50 %) and F (70 %). Sheu and Rosenberg (1995) also supported this theory in their comparison of the surface morphology of ethyl caprylate microcapsules. They also reported that the presence of depressions and surface cracks is inversely related to the WPI content, which slows the drying rate and increases the elasticity of the matrix wall. Additionally, based on the obtained images, treatments prepared with CS walls also resulted in more uniform surfaces with significantly fewer pores than treatments prepared with a combination of WPI and MD.

3.9. Fourier transform infrared spectroscopy (FTIR)

FT-IR spectroscopy is commonly employed to study the composition and structural characteristics of biomaterials. Fig. 3 (a), (b),

and (c) display the FTIR spectra of pure Sargassum extract, microcapsules prepared with CS (at a ratio of 4:1), and microcapsules prepared with WPI and MD. Coarse algal species such as *Sargassum* have high contents of aromatic polyphenol complexes or lignin-like substances [63,64]. In the FTIR spectrum of *Sargassum* extract, absorption bands attributable to aromatic rings are observed in the range of 3150–3000 cm^{-1}, overlapping with OH absorption bands [65]. Thus, the presence of these compounds can be confirmed by absorption bands located between 2900 and 3400 cm^{-1}, corresponding to aromatic ring vibrations [66]. All three examined samples also contained alkene groups, nearly uniformly indicated without alteration by an absorption band between 2840 and 3000 cm^{-1}, representing vinyl C–H bending vibrations in the related plane. This aligns perfectly with studies conducted by Nosrati et al. (2021).

The absorption band at 3306.40 cm^{-1} in *Sargassum* species is due to the presence of aromatic ethers, which are much more pronounced in microcapsules prepared from the CS combination. A comparison of the three spectra revealed that the primary bonds present in the spectrum of the pure *Sargassum* extract, in addition to the O–H bond in the range of 3200–3400 cm^{-1}, were visible in the other FTIR spectra presented. The C-O bonds in the wavelength range of 1000–1100 cm^{-1}, the C-H groups related to CH_2 and CH_3 groups in the wavelength range of 1400, and finally, the C-H groups linked to alkyl groups in the wavelength range of 2800–2900 cm^{-1} in the spectra related to microcapsules (Fig. 3b and c), particularly in the microcapsule with MD and WPI, were removed, which can be attributed to the proper and strong coverage of the wall materials.

Studies conducted by Kushalia et al. (2022) have also removed some of the primary bonds present in the extract in the spectrum of the prepared microcapsule, which is consistent with the present study's results and indicates the accuracy of the fine powder process and the concealment of bonds related to the extract inside the capsules. On the other hand, in the FTIR spectra of microcapsules prepared with a combination of WPI and MD, new bonds, especially from the C-F group, were observed in the wavelength range below 2000 cm^{-1}, indicating greater strength in the formed capsules. Considering that the highest microencapsulation efficiency in this study was related to treatment I, which was prepared with a combination of WPI and MD, this superiority in terms of the quality and performance of the microcapsules prepared with this wall combination compared with those with CS can also be attributed to changes in the structure of the abovementioned bonds in the final prepared microcapsules [63].

3.10. X-ray diffraction (XRD) analysis

X-ray diffraction (XRD) analysis was employed to determine the crystalline structure of optimized microcapsules prepared with different shell compositions and ratios, to investigate the formation of broken and formed bonds during the encapsulation process. The results obtained from the spectra are consistent with those in Fig. 4.

XRD analysis is a nonmicroscopic analytical technique based on X-ray radiation interactions with a sample, revealing scattering patterns in various directions upon the atomic planes of the material. This method provides insights into the crystalline structure of a substance, its grain size, existing phases, lattice constants, defects, residual stresses, and sample composition. In the present study, X-ray diffraction (XRD) was conducted to examine the crystalline structure of microcapsules prepared from the four top-performing treatments based on encapsulation efficiency.

The crystalline quality of the prepared microparticles was confirmed through XRD analysis (Fig. 4). Each spectrum exhibited a main peak with reflections corresponding to treatments F, I, C, and M, at angles of 13.36°, 19.60°, 19.10°, and 19.20°, respectively. Using MATCH software version 3, crystalline structure A was determined for treatment C, which was prepared with 50 % WPI and 50 % MD, and structure T was determined for treatment I, which was prepared with 70 % WPI and 30 % MD. These findings indicate new bonds, particularly from C−F groups below 2000 cm^{-1}, in the FTIR spectra of microcapsules prepared with different shell compositions, highlighting the increased strength of the capsules formed. The highest microencapsulation efficiency was observed in treatment I, which was prepared with 70 % WPI and 30 % MD, suggesting that the quality and performance of the capsules were superior to those of the capsules prepared with CS. This superiority in structural bonds in the final microcapsules was also noted by Ref. [63].

XRD analysis provides information on the degree of crystallinity in semi-crystalline polymers and their structural orientation due to the presence of long chains, allowing for the assessment of polymer properties such as thermal stability and mechanical strength [67]. Unlike mineral solids, which have 100 % crystalline structures, polymers can exhibit various forms, such as highly crystalline, semi-crystalline, microcrystalline, and amorphous forms, each displaying different peak shapes [68]. Therefore, based on the observed XRD peaks, all four treatments resulted in relatively sharp peaks with consistent heights and full width at half maximum (FWHM) values of approximately 4–6, indicating their crystalline structure. The recorded XRD patterns correlate with findings from studies by Ref. [69], who demonstrated that silver nanoparticles synthesized from *Sargassum muticum* aqueous extract have a nano-crystalline nature.

4. Conclusion

In this work, it was possible to evaluate the performance of different wall material combinations in SIE microencapsulation by freeze-drying. The MD:WPI combination resulted in the best encapsulation efficiency. On the other hand, supplementary tests, such as the evaluation of physicochemical properties like solubility, stability, density, and phenol content, revealed better performance of the MD: WPI combination than CS for SIE encapsulation. Considering the high phenolic content of *Sargassum* extract and its acceptable encapsulation in this research, studying its antioxidant effects on products sensitive to oxidation can be very useful.

CRediT authorship contribution statement

Seyed Saeed Sekhavatizadeh: Writing – original draft, Methodology. **Mohammad Ganje:** Writing – review & editing,

Supervision, Software, Conceptualization. **Seyedeh Sedigheh Hashemi:** Funding acquisition, Data curation. **Mohammad Reza Mozafarian:** Data curation.

Ethical review

This study does not involve any human or animal testing.

Data availability

The data will be made available upon reasonable request.

Funding statement

This research did not receive any specific grant from funding agencies in the public, commercial, or not-for-profit sectors.

Declaration of competing interest

The authors declare that they have no known competing financial interests or personal relationships that could have appeared to influence the work reported in this paper.

Acknowledgments

The authors thank the head of the Fars Agriculture Research and Education Center for his support and encouragement in carrying out the work.

References

[1] R. Hima, S. Harikrishnan, M. Parivallal, M.S. Abdul Rahman, S.M. Basha, K. Sreedhar, P.J. Anantharaman, Analysis of the chemical, nutrient and physicochemical properties of brown macroalgae, Sargassum ilicifolium collected from Mandapam Coast, Rameshwaram, Biochemical Cellular Archives 23 (2) (2023) 1029, https://doi.org/10.51470/bca.2023.23.2.1029.

[2] S.G. Widyaswari, M. Metusalach, K. Kasmiati, N. Amir, Bioactive compounds and DPPH antioxidant activity of underutilized macroalgae (Sargassum spp.) from coastal water of Makassar, Indonesia, Biodiversitas Journal of Biological Diversity 25 (2024) 162–168, https://doi.org/10.13057/biodiv/d250118.

[3] P. Akbary, A. Ajdari, B. Ajang, Growth, survival, nutritional value and phytochemical, and antioxidant state of Litopenaeus vannamei shrimp fed with premix extract of brown Sargassum ilicifolium, Nizimuddinia zanardini, Cystoseira indica, and Padina australis macroalgae, Aquacult. Int. 31 (2023) 681–701, https://doi.org/10.1007/s10499-022-00994-5.

[4] A.D. Premarathna, R. Tuvikene, M. Somasiri, M. De Silva, R. Adhikari, T. Ranahewa, R. Wijesundara, S. Wijesekera, I. Dissanayake, P.J. Wangchuk, A novel therapeutic effect of mannitol-rich extract from the brown seaweed Sargassum ilicifolium using in vitro and in vivo models, BMC Complementary Medicine Therapies 23 (2023) 1–17, https://doi.org/10.1186/s12906-023-03879-z.

[5] A. Roa-Tort, O.G. Meza-Márquez, G. Osorio-Revilla, T. Gallardo-Velázquez, O.A. Ramos-Monroy, Extraction and microencapsulation of phytochemical compounds from mango peel (Mangifera indica L.) var."Kent" and assessment of bioaccessibility through in vitro digestion, Processes 12 (2024) 1–19, https://doi.org/10.3390/pr12010154.

[6] D.G. Bortolini, G.M. Maciel, C.W.I. Haminiuk, Edible bubbles: a delivery system for enhanced bioaccessibility of phenolic compounds in red fruits and edible flowers, Innovative Food Sci. Emerging Technol. 91 (2024) 103523.

[7] H. Andishmand, M. Yousefi, N. Jafari, S. Azadmard-Damirchi, A. Homayouni-Rad, M. Torbati, H. Hamishehkar, Designing and fabrication of colloidal nano-phytosomes with gamma-oryzanol and phosphatidylcholine for encapsulation and delivery of polyphenol-rich extract from pomegranate peel, Int. J. Biol. Macromol. 256 (2024) 128501, https://doi.org/10.1016/j.ijbiomac.2023.128501.

[8] R. Zhang, T. Belwal, L. Li, X. Lin, Y. Xu, Z. Luo, Recent advances in polysaccharides stabilized emulsions for encapsulation and delivery of bioactive food ingredients: a review, Carbohydrate Polymers 242 (2020) 1–82, https://doi.org/10.1016/j.carbpol.2020.116388.

[9] F. Borhanpour, S.S. Sekhavatizadeh, S. Hosseinzadeh, M. Hasanzadeh, M.-T. Golmakani, M. Moharreri, Effect of microencapsulated chavil (Ferulago angulata) extract on physicochemical, microbiological, textural and sensorial properties of UF-feta-type cheese during storage time, Int. J. Food Eng. 18 (2021) 53–66, https://doi.org/10.1515/ijfe-2021-0198.

[10] S. Fatemeh, F. Soltaninejad, S.S. Sekhavatizadeh, Effects of encapsulated black caraway extract and sesame oil on kolompeh quality, Foods and Raw Materials 7 (2019) 311–320, https://doi.org/10.21603/2308-4057-2019-2-311-320.

[11] E. Rahpeyma, S.S. Sekhavatizadeh, Department of scientific and publishing activities, Foods and Raw Materials 8 (2020) 40–51, https://doi.org/10.21603/2308-4057-2020-1-40-51.

[12] S.S. Sekhavatizadeh, K. Banisaeed, M. Hasanzadeh, S. Khalatbari-Limaki, H. Amininezhad, Physicochemical properties of kashk supplemented with encapsulated lemongrass extract, Foods and Raw Materials 11 (2023) 141–151, https://doi.org/10.21603/2308-4057-2023-1-560.

[13] A. Rezvankhah, Z. Emam-Djomeh, G. Askari, Encapsulation and delivery of bioactive compounds using spray and freeze-drying techniques: a review, Dry. Technol. 38 (2020) 235–258, https://doi.org/10.1080/07373937.2019.1653906.

[14] P. Schuck, R. Jeantet, B. Bhandari, X.D. Chen, I.T. Perrone, A.F. de Carvalho, M. Fenelon, P. Kelly, Recent advances in spray drying relevant to the dairy industry: a comprehensive critical review, Dry. Technol. 34 (2016) 1773–1790, https://doi.org/10.1080/07373937.2016.1233114.

[15] N. Wang, C. Wang, X. Gao, X. Zhao, H. Wei, J. Luo, X. You, H. Jiang, X. Zhang, C. Yuan, DHA-mediated milk protein treated by ultrasound-assisted pH-shifting for enhanced astaxanthin delivery and processed cheese application, J. Dairy Sci. (2024), https://doi.org/10.3168/jds.2023-24342 [In Press].

[16] S.A. Ledri, J.M. Milani, S.-A. Shahidi, A.J.F.C.X. Golkar, Comparative analysis of freeze drying and spray drying methods for encapsulation of chlorophyll with maltodextrin and whey protein isolate. https://doi.org/10.1016/j.fochx.2024.101156, 2024.

[17] D.W. Dadi, S.A. Emire, A.D. Hagos, J.-B. Eun, Physical and functional properties, digestibility, and storage stability of spray-and freeze-dried microencapsulated bioactive products from Moringa stenopetala leaves extract, Industrial Crops Products 156 (2020) 112891, https://doi.org/10.1016/j.indcrop.2020.112891.

[18] M.F. Manzoor, M.T. Afraz, B.B. Yılmaz, M. Adil, N. Arshad, G. Goksen, M. Ali, X.-A. Zeng, Recent progress in natural seaweed pigments: green extraction, health-promoting activities, techno-functional properties and role in intelligent food packaging, Journal of Agriculture and Food Research 15 (2024) 100991, https://doi.org/10.1016/j.jafr.2024.100991.

[19] S.F. Mohammadi Kabari, H.A. Asadi-Gharneh, V. Tavallali, V. Rowshan, Differential response of biochar in mitigating salinity stress in periwinkle (Catharanthus roseus L.) as an ornamental-medicinal plant species, Int. J. Phytoremediation 94 (2024) 1–12, https://doi.org/10.1080/15226514.2023.2300115.

[20] Z. Ghanbarzadeh, S. Mohsenzadeh, V. Rowshan, M.J. Zarei, Mitigation of water deficit stress in Dracocephalum moldavica by symbiotic association with soil microorganisms, Sci. Hortic. 272 (2020) 109549, https://doi.org/10.1016/j.scienta.2020.109549.

[21] T. Zhang, M. Ding, X. Wang, J. Zhong, Droplet and creaming stability of fish oil-loaded gelatin/surfactant-stabilized emulsions depends on both the adsorption ways of emulsifiers and the adjusted pH, Food Sci. Hum. Wellness 9 (2020) 280–288, https://doi.org/10.1016/j.fshw.2020.04.002.

[22] J.S. e Silva, D. Splendor, I. Gonçalves, P. Costa, J. Sousa Lobo, Note on the measurement of bulk density and tapped density of powders according to the European Pharmacopeia, AAPS PharmSciTech 14 (2013) 1098–1100, https://doi.org/10.1208/s12249-013-9994-5.

[23] R.K. Lekshmi, M. Rahima, N. Chatterjee, C. Tejpal, K. Anas, K. Vishnu, K. Sarika, K. Asha, R. Anandan, M. Suseela, Chitosan-Whey protein as efficient delivery system for squalene: characterization and functional food application, Int. J. Biol. Macromol. 135 (2019) 855–863, https://doi.org/10.1016/j.ijbiomac.2019.05.153.

[24] F. Borhanpour, S.S. Sekhavatizadeh, S. Hosseinzadeh, M. Hasanzadeh, M.-T. Golmakani, M. Moharreri, Effect of microencapsulated chavil (Ferulago angulata) extract on physicochemical, microbiological, textural and sensorial properties of UF-feta-type cheese during storage time, Int. J. Food Eng. 18 (2021) 53–66, https://doi.org/10.1515/ijfe-2021-0198.

[25] M.D. Catarino, R. Silva-Reis, A. Chouh, S. Silva, S.S. Braga, A.M. Silva, S.M. Cardoso, Applications of antioxidant secondary metabolites of sargassum spp, Mar. Drugs 21 (2023) 172, https://doi.org/10.3390/md21030172.

[26] H.C. Carneiro, R.V. Tonon, C.R. Grosso, M.D. Hubinger, Encapsulation efficiency and oxidative stability of flaxseed oil microencapsulated by spray drying using different combinations of wall materials, J. Food Eng. 115 (2013) 443–451, https://doi.org/10.1016/j.jfoodeng.2012.03.033.

[27] K. Ganapathi, V. Subramanian, S. Mathan, Bioactive potentials of brown seaweeds, Sargassum myriocystum J. Agardh S. plagiophyllum C. Agardh and S. ilicifolium (Turner) J. Agardh, Int. Res. J. Pharmaceut. Appl. Sci. 3 (2013) 105–111.

[28] M. Akhtar, E. Dickinson, Whey protein-maltodextrin conjugates as emulsifying agents: an alternative to gum Arabic, Food Hydrocolloids 21 (2007) 607–616, https://doi.org/10.1016/j.foodhyd.2005.07.014.

[29] H. Mirhosseini, C.P. Tan, N.S. Hamid, S. Yusof, Effect of Arabic gum, xanthan gum and orange oil contents on ζ-potential, conductivity, stability, size index and pH of orange beverage emulsion, Colloids Surf. A Physicochem. Eng. Asp. 315 (2008) 47–56, https://doi.org/10.1016/j.colsurfa.2007.07.007.

[30] H. Chen, S. Iqbal, P. Wu, R. Pan, N. Wang, R.A. Bhutto, W. Rehman, X.D. Chen, Enhancing rheology and reducing lipid digestion of oil-in-water emulsions using controlled aggregation and heteroaggregation of soybean protein isolate-peach gum microspheres, Int. J. Biol. Macromol. 273 (2024) 132964, https://doi.org/10.1016/j.ijbiomac.2024.132964.

[31] A. Gomes, A.L.R. Costa, L.H. Fasolin, E.K. Silva, Rheological properties, microstructure, and encapsulation efficiency of inulin-type dietary fiber-based gelled emulsions at different concentrations, Carbohydrate Polymers 347 (2025) 122742, https://doi.org/10.1016/j.carbpol.2024.122742.

[32] J. Cai, R. Lopez, Y. Lee, Effect of feed material properties on microencapsulation by spray drying with a three-fluid nozzle: soybean oil encapsulated in maltodextrin and sugar beet pectin, J. Food Process. Preserv. 2023 (2023) 4974631, https://doi.org/10.1155/2023/4974631.

[33] A. Soottitantawat, F. Bigeard, H. Yoshii, T. Furuta, M. Ohkawara, P. Linko, Influence of emulsion and powder size on the stability of encapsulated D-limonene by spray drying, Innovat. Food Sci. Emerg. Technol. 6 (2005) 107–114, https://doi.org/10.1016/j.ifset.2004.09.003.

[34] M.V. Bule, R.S. Singhal, J.F. Kennedy, Microencapsulation of ubiquinone-10 in carbohydrate matrices for improved stability, Carbohydrate polymers 82 (2010) 1290–1296, https://doi.org/10.1016/j.carbpol.2010.07.012.

[35] S. Zeidvand, S. Movahhed, H. Ahmadi Chenarbon, P. Rajaei, Encapsulation of felty germander (Teucrium polium L.) extract using the freeze-drying method, Food Sci. Nutr. 12 (7) (2024) 4899–4913, https://doi.org/10.1002/fsn3.4136.

[36] L.R. Kumar, N. Chatterjee, C. Tejpal, K. Vishnu, K. Anas, K. Asha, R. Anandan, S. Mathew, Evaluation of chitosan as a wall material for microencapsulation of squalene by spray drying: characterization and oxidative stability studies, Int. J. Biol. Macromol. 104 (2017) 1986–1995, https://doi.org/10.1016/j.ijbiomac.2017.03.114.

[37] C. Belingheri, B. Giussani, M.T. Rodriguez-Estrada, A. Ferrillo, E. Vittadini, Oxidative stability of high-oleic sunflower oil in a porous starch carrier, Food Chem. 166 (2015) 346–351, https://doi.org/10.1016/j.foodchem.2014.06.029.

[38] N.E. Rahmani-Manglano, M.L. Andersen, E.M. Guadix, P.J. García-Moreno, Oxidative stability and oxygen permeability of oil-loaded capsules produced by spray-drying or electrospraying measured by electron spin resonance, Food Chem. 430 (2024) 136894, https://doi.org/10.1016/j.foodchem.2023.136894.

[39] K. Šavikin, N. Nastić, T. Janković, D. Bigović, B. Miličević, S. Vidović, N. Menković, J. Vladić, Effect of type and concentration of carrier material on the encapsulation of pomegranate peel using spray drying method, Foods 10 (2021), https://doi.org/10.3390/foods10091968, 1968.

[40] E. Macías-Cortés, J. Gallegos-Infante, N. Rocha-Guzmán, M. Moreno-Jiménez, L. Medina-Torres, R. González-Laredo, Microencapsulation of phenolic compounds: technologies and novel polymers, Rev. Mex. Ing. Quim. 19 (2020) 491–521, https://doi.org/10.24275/rmiq/Alim642.

[41] M. Zhao, W. Cao, L. Li, A. Ren, Y. Ang, J. Chen, B. Bhandari, Z. Wang, X. Ren, G. Ren, Effects of different proteins and maltodextrin combinations as wall material on the characteristics of Cornus officinalis flavonoids microcapsules, Front. Nutr. 9 (2022) 1007863, https://doi.org/10.3389/fnut.2022.1007863.

[42] S. Kaveh, A. Sadeghi Mhoonak, K. Sarabandi, Z. Graeely, Spray drying of stevia extract: evaluation of physicochemical, functional and microstructural properties, Innovative Food Technologies 5 (2018) 637–650.

[43] B. Bhandari, N. Bansal, M. Zhang, P. Schuck, Handbook of Food Powders: Processes and Properties, Elsevier, 2023.

[44] A. Halahlah, V. Piironen, K.S. Mikkonen, T.M. Ho, Polysaccharides as wall materials in spray-dried microencapsulation of bioactive compounds: physicochemical properties and characterization, Crit. Rev. Food Sci. Nutr. 63 (2023) 6983–7015, https://doi.org/10.1080/10408398.2022.2038080.

[45] K. Maroof, R.F. Lee, L.F. Siow, B.H. Goh, K.F. Chen, S.H. Gan, The effects of drying methods and leucine addition on properties of propolis powder: towards the development of a new formulation, Food Chemistry Advances 3 (2023) 100449, https://doi.org/10.1016/j.focha.2023.100449.

[46] Y. Zahedi, R. Shaddel, M. Salamatian, A. Szumny, Nanoliposomal encapsulation of Capparis spinosa extract and its application in jelly formulation, Molecules 29 (2024) 2804, https://doi.org/10.3390/molecules29122804.

[47] V. Anand, V. Ksh, A. Kar, E. Varghese, S. Vasudev, C. Kaur, Encapsulation efficiency and fatty acid analysis of chia seed oil microencapsulated by freeze-drying using combinations of wall material, Food Chem. 430 (2024) 136960, https://doi.org/10.1016/j.foodchem.2023.136960.

[48] E. Díaz-Montes, Wall materials for encapsulating bioactive compounds via spray-drying: a review, Polymers 15 (2023) 2659, https://doi.org/10.3390/polym15122659.

[49] A. Qayum, A. Rashid, Q. Liang, Y. Wu, Y. Cheng, L. Kang, Y. Liu, C. Zhou, M. Hussain, X. Ren, Ultrasonic and homogenization: an overview of the preparation of an edible protein-polysaccharide complex emulsion, Compr. Rev. Food Sci. Food Saf. 22 (2023) 4242–4281, https://doi.org/10.1111/1541-4337.13221.

[50] P. Shao, S. Xuan, W. Wu, L. Qu, Encapsulation efficiency and controlled release of Ganoderma lucidum polysaccharide microcapsules by spray drying using different combinations of wall materials, Int. J. Biol. Macromol. 125 (2019) 962–969, https://doi.org/10.1016/j.ijbiomac.2018.12.153.

[51] I. Khalifa, M. Li, T. Mamet, C. Li, Maltodextrin or gum Arabic with whey proteins as wall-material blends increased the stability and physiochemical characteristics of mulberry microparticles, Food Biosci. 31 (2019) 100445, https://doi.org/10.1016/j.fbio.2019.100445.

[52] L. Fan, Y. Liu, S. Huang, J. Li, Effects of proteins on emulsion stability: the role of proteins at the oil-water interface, Food Chem. 397 (2022) 133726, https://doi.org/10.1016/j.foodchem.2022.133726.

[53] J. Yang, P. Shen, A. de Groot, H.C. Mocking-Bode, C.V. Nikiforidis, L.M. Sagis, Oil-water interface and emulsion stabilising properties of rapeseed proteins napin and cruciferin studied by nonlinear surface rheology, J. Colloid Interface Sci. 662 (2024) 192–207, https://doi.org/10.1016/j.jcis.2024.02.030.

[54] Ö. Altay, Ö. Köprüalan, I. İlter, M. Koç, F.K. Ertekin, S.M. Jafari, Spray drying encapsulation of essential oils; process efficiency, formulation strategies, and applications, Crit. Rev. Food Sci. Nutr. 64 (2024) 1139–1157, https://doi.org/10.1080/10408398.2022.2113364.

[55] C. Jansen-Alves, F.N. Victoria, C.D. Borges, R.C.J. Zambiazi, Encapsulation of propolis extract in ovalbumin protein particles: characterization and in vitro digestion, Nat. Prod. Res. 38 (2024) 1766–1770, https://doi.org/10.1080/14786419.2023.2214945.

[56] M. Jumaa, B.W. Müller, The effect of oil components and homogenization conditions on the physicochemical properties and stability of parenteral fat emulsions, Int. J. Pharm. 163 (1998) 81–89, https://doi.org/10.1016/S0378-5173(97)00369-4.

[57] O. Sarheed, M. Dibi, K.V. Ramesh, Studies on the effect of oil and surfactant on the formation of alginate-based O/W lidocaine nanocarriers using nanoemulsion template, Pharmaceutics 12 (2020) 1223, https://doi.org/10.3390/pharmaceutics12121223.
[58] M. Li, H. Yu, M.-A. Gantumur, L. Guo, L. Lian, B. Wang, C. Yu, Z. Jiang, Insight into oil-water interfacial adsorption of protein particles towards regulating pickering emulsions: a review, Int. J. Biol. Macromol. (2024) 132937, https://doi.org/10.1016/j.ijbiomac.2024.132937.
[59] S.M. Jafari, E. Assadpoor, Y. He, B. Bhandari, Encapsulation efficiency of food flavours and oils during spray drying, Dry. Technol. 26 (2008) 816–835, https://doi.org/10.1080/07373930802135972.
[60] Y. Tao, Z. Tang, Q. Huang, X. Xu, X. Cheng, G. Zhang, X. Jing, X. Li, J. Liang, D. Granato, Effects of spray drying temperature on physicochemical properties of grapeseed oil microcapsules and the encapsulation efficiency of pterostilbene, LWT 193 (2024) 115779, https://doi.org/10.1016/j.lwt.2024.115779.
[61] R. Indrawati, H. Sukowijoyo, R.D.E. Wijayanti, L. Limantara, Encapsulation of brown seaweed pigment by freeze drying: characterization and its stability during storage, Procedia Chem. 14 (2015) 353–360, https://doi.org/10.1016/j.proche.2015.03.048.
[62] S. Aghajanzadeh, A. Sultana, A.M. Ziaiifar, S. Khalloufi, Formation of pores and bubbles and their impacts on the quality attributes of processed foods: a review, Food Res. Int. (2024) 114494, https://doi.org/10.1016/j.foodres.2024.114494.
[63] M. Haji Abolhasani, Extraction and purification of alginic acid from brown algae on the east southern coast of Iran, J. Plant Res. 34 (2021) 543–559.
[64] L. Alzate-Gaviria, J. Domínguez-Maldonado, R. Chablé-Villacís, E. Olguin-Maciel, R.M. Leal-Bautista, G. Canché-Escamilla, A. Caballero-Vázquez, C. Hernández-Zepeda, F.A. Barredo-Pool, R. Tapia-Tussell, Presence of polyphenols complex aromatic "lignin" in sargassum spp. from Mexican caribbean, J. Mar. Sci. Eng. 9 (2020) 6, https://doi.org/10.3390/jmse9010006.
[65] J.L. López-Miranda, G.A. Molina, R. Esparza, M.A. González-Reyna, R. Silva, M. Estévez, Green synthesis of homogeneous gold nanoparticles using sargassum spp. Extracts and their enhanced catalytic activity for organic dyes, Toxics 9 (2021) 280, https://doi.org/10.3390/toxics9110280.
[66] S. Ali Alhaidrai, F. Al-Hadi, A. Al-Kaf, A.-D. Taj, A. Phytochemical, Screening by FTIR spectroscopic analysis in the methanolic extracts coffee (C. Arabica. L) to seeds and peels (unroasted and roasted) cultivars grown in Yemen, Bioequiv. Bioavailab. Int. J (6) (2022) 000179, https://doi.org/10.23880/beba-16000179.
[67] Z. Yan, A. Zaoui, F. Zaïri, Crystallization and mechanical behavior of semi-crystalline polyethylene, Phys. Scripta 96 (2021) 125729, https://doi.org/10.1088/1402-4896/ac3a4f.
[68] İ. Uzun, Methods of determining the degree of crystallinity of polymers with X-ray diffraction: a review, J. Polym. Res. 30 (2023) 394, https://doi.org/10.1007/s10965-023-03744-0.
[69] S. Azizi, F. Namvar, M. Mahdavi, M.B. Ahmad, R. Mohamad, Biosynthesis of silver nanoparticles using brown marine macroalga, Sargassum muticum aqueous extract, Materials 6 (2013) 5942–5950, https://doi.org/10.3390/ma6125942.